Hand Based Biometry

Erdem Yörük, Helin Dutağacı, Bülent Sankur

Electrical and Electronic Engineering Department, Boğaziçi University, Bebek, İstanbul, Turkey
[erdem.yoruk, dutagach, sankur]@boun.edu.tr
Telephone: (90) 212 359 6414, Fax: (90) 212 287 2465
Corresponding author: Bülent Sankur

ABSTRACT

A biometric scheme based on the silhouettes and/or textures of the hands is developed. The crucial part of the algorithm is the accurate registration of the deformable shape of the hands since subjects are not constrained in pose or posture during acquisition. A host of shape and texture features are comparatively evaluated, such as Independent component features (ICA features), Principal Component Analysis (PCA features), Angular Radial Transform (ART features) and the distance transform (DT) based features. Even with a limited number of training data it is shown that this biometric scheme can perform reliably for populations up to several hundreds.

1. INTRODUCTION

Hand shape and hand texture is an emerging new modality in biometry. It possesses certain advantages over the more established competitor techniques, in that its acquisition is less cumbersome and more user-friendly. Furthermore it is much less susceptible to intrinsic variations and environmental artifacts [1]. In contrast, fingerprint acquisition is usually associated for criminal identification, and is therefore psychologically disturbing. Iris and retinal scans require sophisticated, expensive and more intrusive acquisition systems. Systems relying on human face or voice identification are more established at present, and seem user-friendlier, but suffer severely from intra-class variations and background/noise elimination problems. For example, face recognition is handicapped by artifacts of pose, expression, accessories and illumination. Therefore, hand-based person identification/verification systems provide an attractive and growing alternative biometric scheme [2], that can be used either singly or in cooperation with other evidences in a multimodal scheme.

Previous investigations on hand-based biometry have geometrical properties of parts and/or of the whole or texture. Schemes that utilize *geometrical features* of the hand focus on such characteristics as widths of fingers at articulations, finger and palm lengths, finger deviations and the angles of the inter-finger valleys with the horizontal [3] [4], [5], [6]. Oden et al. [7] use jointly finger *shape information and geometric features*. The shape information of the individual fingers (but not the whole hand) was extracted via implicit polynomials and the geometric features were joined at the feature fusion stage.

There is also increasing research on *palm print-based* identification/verification systems. One challenging problem with the palm print is the extraction of features such as line structures from the palm print image. For that reason, most of the proposed algorithms [8], [9], [10] require ink markings for obtaining enhanced palm print images. On the other hand, Zhan [8], [11] uses a special scanning system to automatically extract the palm curves from high-quality and well-aligned palm print images. The verification algorithm proposed by Han et al. [12] does not require peg or ink usage, and the palm print features. In Kong et al. [13] 2-D Gabor filters are implemented to obtain texture information and two palm print images are compared in terms of their hamming distance. Kumar [14] uses both texture and shape information.

In this work we propose a hand-based biometric system, which is original in two respects. Our first contribution is the development of a very accurate hand normalization scheme, whereby hand images captured in arbitrary postures and poses are registered to a standard pose and posture. This stage is crucial in that it enables the employment of global features and increases the population size considerably for which accurate identification and verification is possible. Our second contribution is the comparative assessment of various feature sets. Two of these features are data-driven

Image and Video Communications and Processing 2005, edited by Amir Said,
John G. Apostolopoulos, Proc. of SPIE-IS&T Electronic Imaging,
SPIE Vol. 5685 © 2005 SPIE and IS&T · 0277-786X/05/$15

statistical features, namely principal components and independent components, and two of them are general features, namely, axial radial transform and distance transform. Furthermore we compare the performance of the biometric algorithm with these features as applied to pure hand shape (binary silhouette) and to the textured hand shape (gray level palm texture within the hand contour boundary). We remark that the size of the enrollment in our work exceeds the populations used in the literature by almost an order of magnitudes. Finally we investigate the effect of the time lapse, that is the performance differential when the time interval between training acquisition and test acquisition is at least six months.

The paper is organized as follows: Section 2 describes pose normalization of hands. Section 3 deals with the extraction of global features, namely principal components, independent components, angular radial transform coefficients and distance transform-based features. In section 4 we give the experimental results. Finally section 5 concludes our work.

2. SHAPE NORMALIZATION OF HANDS

Fig. 1 shows various hands in different orientations and finger postures. Notice that during the image acquisition there are no constraints like pegs, with the sole requirement that the fingers should stay apart. After segmentation of the hands from its background, first task is to normalize the shape of the hands, that is re-orient the fingers to pre-determined directions, and register the overall hand to a fixed location and orientation. Since hands are deformable organs this registration of the deformable hand shape becomes the most crucial step in the recognition and verification tasks. For this purpose, the hand is first subjected to a global translation and rotation. Then fingers are first localized based on the hand contour data using the finger tips and valleys. These nine anatomic extremities can be robustly found on the radial distance sequence of the hand contour with respect some origin point around the wrist. Any artifacts on the fingers, like rings, are removed. Each finger is brought to its normalized orientation by rotating it around the metacarpal-phalanx joint. The locations of these joints, hidden under the palm, are initialized with those of a proto-hand with known pivot locations. The pivot locations are first adapted to the actual hand with a scaling transformation, where we use the horizontal palm width and the middle finger lengths as gauges. Subsequently the updated pivots are projected onto the extension of the major axis of the finger. These processing steps, as illustrated in Fig. 2, yield as output the binary hand silhouette as well as the color-corrected hand texture of both palm and fingers superimposed on the silhouette [15].

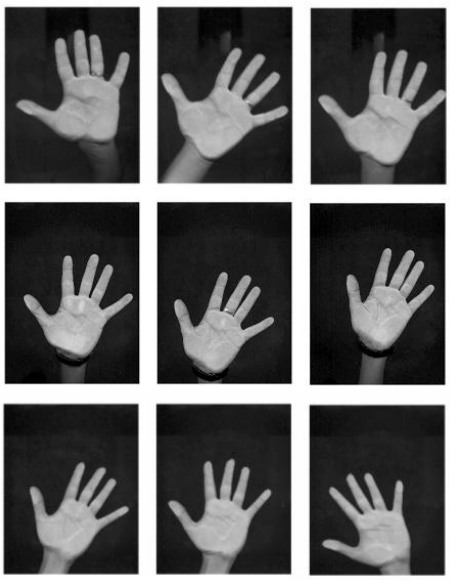

Figure 1. Each row: Images of the left hand of a subject in different postures

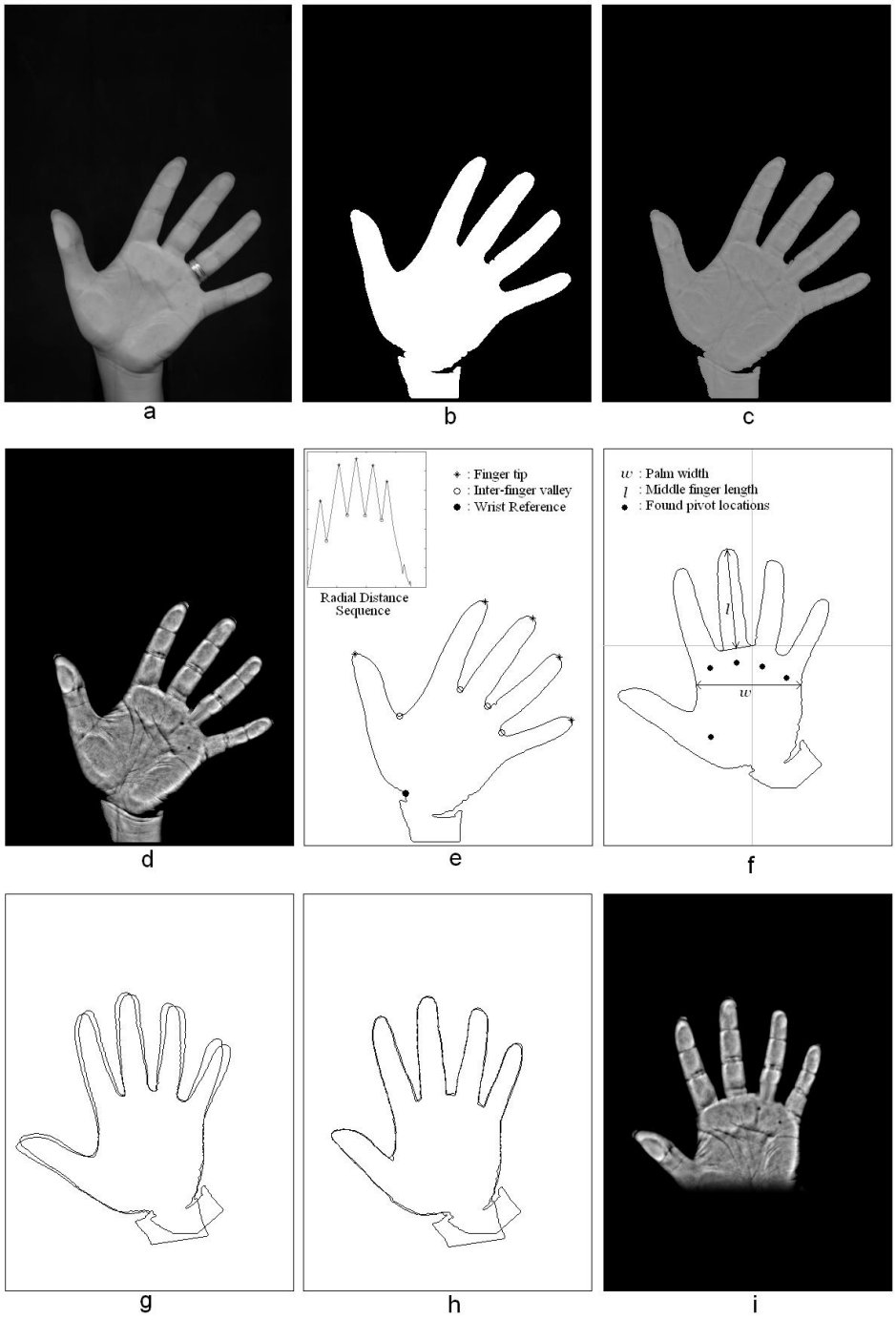

Figure 2. Processing steps for hand normalization: **a)** Original hand image; **b)** Segmented hand image; **c)** Illumination corrected hand image (ring removed); **d)** Gray-scale, texture enhanced hand image; **e)** Determination of finger tips and valleys; **f)** Initial global registration by translation and rotation: Middle finger length and palm width for hand image scaling and derivation of the metacarpal pivots; **g)** Superposed contours taken from different sessions of the same individual with rigid hand registration only; **h)** Superposed contours taken from different sessions of the same individual after finger orientation normalization; **i)** Final gray-scale, normalized hand with cosine-attenuated wrist.

3. FEATURE EXTRACTION AND RECOGNITION

We have considered several feature sets in order to accomplish biometric identification and verification tasks. Some of these utilize pure shape information ass given by the silhouette while others make use of both the shape and the circumscribed texture information. The ones that apply to shape only are independent components analysis features (ICA), principal components analysis features (PCA), axial radial transform features (ART) and distance transform features (DT). In a previous study, we had considered weighted Haussdorff distance as well, but we have excluded it from the competition as its performance falls short of the above ones [15]. The features that make use of both the shape and texture information are the ICA, PCA and ART schemes.

3.1. ICA features [18, 19]

The Independent Component Analysis (ICA) is a technique for extracting statistically independent variables from mixtures. Generally, one assumes that each observed signal $\{x(k), k = 1,..., K\}$ consists a mixture of a set of N unknown independent source signals $\{s(k), k = 1,..., K\}$, mixed through an unknown mixing matrix **A**. With x_i and s_i (i=1,…,N) forming the rows of the N×K matrices **X** and **S**, respectively, we have the following model: $\mathbf{X} = \mathbf{AS}$. Here **X** is the set of recorded hand images and is made up of lexicographically ordered hand image pixels. The dimension of these vectors is K (for example, K = 40,000, if we assume a 200×200 hand image). The ICA algorithm finds a linear transformation **W** that minimizes the statistical dependence between the output components y_i, that correspond to hypothesized independent sources s_i: $\hat{\mathbf{S}} = \mathbf{Y} = \mathbf{WX}$. We have used the fastICA algorithm to find the separating or de-mixing matrix **W**. The fastICA algorithm maximizes the statistical independence between the output components using maximization of their negentropy. The resulting independent "hand sources" are shown in Fig. 3.

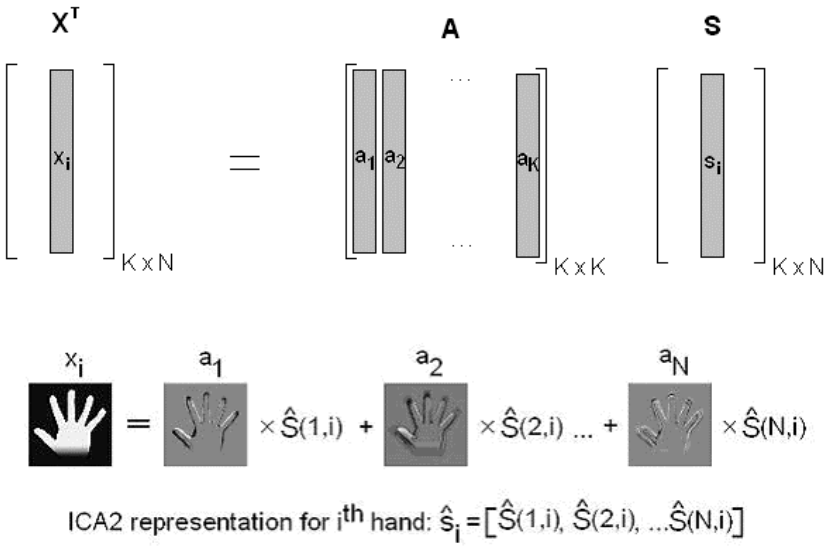

Figure 3. Hand pattern synthesis using ICA2 basis functions. a_i, i = 1,…, N denote the N basis images, while the weighting coefficients S(n,i), i = 1,…, N for the hand i are statistically independent

3.2. PCA features [16, 17]

For the implementation of PCA, each hand shape is first converted to one-dimensional contour vector. We have used finger tips and valleys as landmarks and re-sampled the intervening contour segments in order to establish correspondence among the contour elements. We obtain an eigenspace with the PCA eigenvectors, and the projection of

a hand contour onto this eigenspace constitutes the feature set of that hand. The modes of variation obtained from PCA exhibit interesting characteristics as illustrated in Fig. 4. The dimension of the eigenspace, i.e. the number of features, is an important parameter and is analyzed through tests. We have also applied PCA to the normalized hand images to make use of appearance information residing at the fingers and the palm.

Range of i^{th} coefficient	Modes of variation	Range of i^{th} coefficient	Modes of variation
1st mode $\pm 2\sqrt{\lambda_1}$	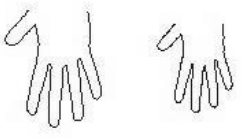 Scale of hands	**6th mode** $\pm 6\sqrt{\lambda_6}$	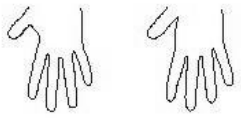 Shape of the thumb valley
2nd mode $\pm 4\sqrt{\lambda_2}$	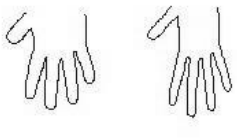 Elongation of hands	**7th mode** $\pm 6\sqrt{\lambda_7}$	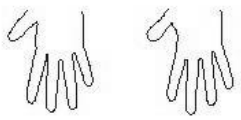 Shape of the thumb
3rd mode $\pm 6\sqrt{\lambda_3}$	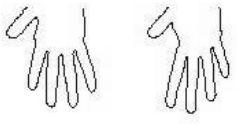 Relative lengths of the fingers	**8th mode** $\pm 7\sqrt{\lambda_8}$	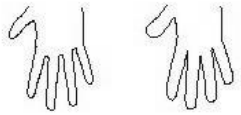 Finger widths relative to the palm width
4th mode $\pm 8\sqrt{\lambda_4}$	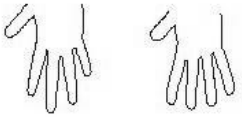 Lengths of index and little fingers and sharpness of the finger tips	**9th mode** $\pm 8\sqrt{\lambda_9}$	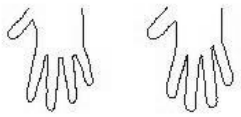 Relative positions of little finger with respect to the palm
5th mode $\pm 6\sqrt{\lambda_5}$	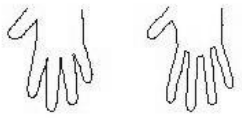 Sharpness of the finger valleys and thinning of fingers.	**10th mode** $\pm 8\sqrt{\lambda_{10}}$	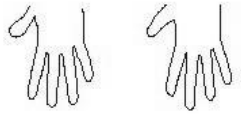 Shape of the thumb

Figure 4. Effect of varying the weights of the first ten eigenvectors.

3.3. ART features [20]

Angular radial transform (ART) is a complex transform defined on the unit disk. The basis functions $V_{nm}(\rho,\theta)$ are defined in polar coordinates as a product of two separable functions along the angular and radial directions:

$$V_{nm}(\rho,\theta) = A_m(\theta)R_n(\rho)$$

where

$$A_m(\theta) = \frac{1}{2\pi}\exp(jm\theta) \qquad \text{and} \qquad R_n(\rho) = \begin{cases} 1 & n = 0 \\ 2\cos(\pi n\rho) & n \neq 0 \end{cases}$$

Notice that variables n = 1..N and m = 1..M represent, respectively, the order along the angular and radial directions. In our work, the Angular Radial Transform is applied either to the binary image of the hands or to the textured hand image. We have used as features the absolute values of the ART coefficients, that is, the inner product of the hand image with the basis functions. These ART basis functions are shown in Fig. 5.

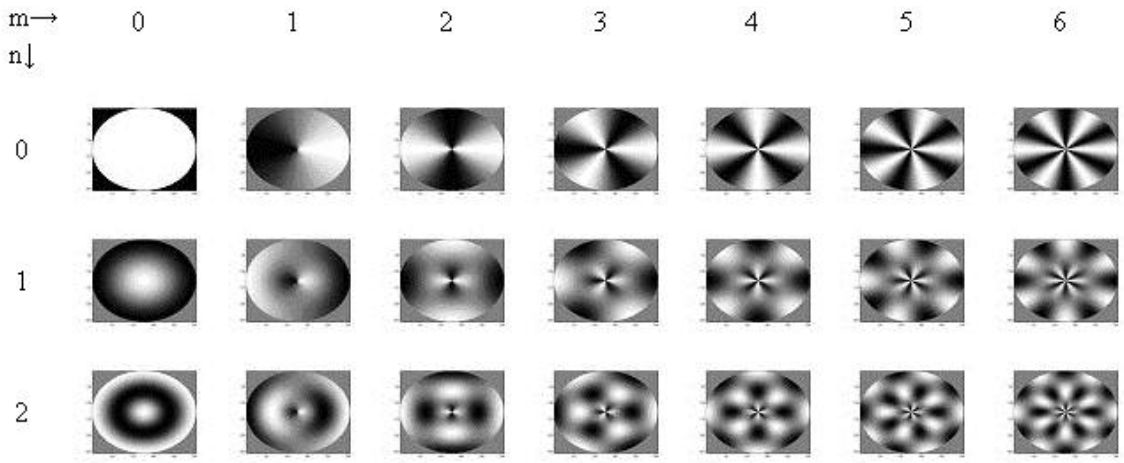

Figure 5. Real parts of ART basis functions.

3.4. DT features

Funkhouser et al. [21] have introduced an interesting set of features applicable in both 2D and 3D shape analyses. The features consist of the "mass" of the shape cut from concentric circles and spheres, respectively, in 2D and 3D cases. To enrich the information, first the distance transform of the hand silhouette is obtained. Then concentric circles around the center of the hand object are defined. The mass resting on each of these circles can be viewed as a one-dimensional periodic function. For each circle of a different radius, the DFT of the mass function is calculated. Finally a 2D signature is obtained for each hand, where one dimension is the radius of the circle and the other dimension is the Fourier coefficient index. Typically a few low order Fourier coefficients are considered. The distance of two hands is defined as the L_1 norm of the difference of their signatures. The sequence of operations are shown in Fig. 6.

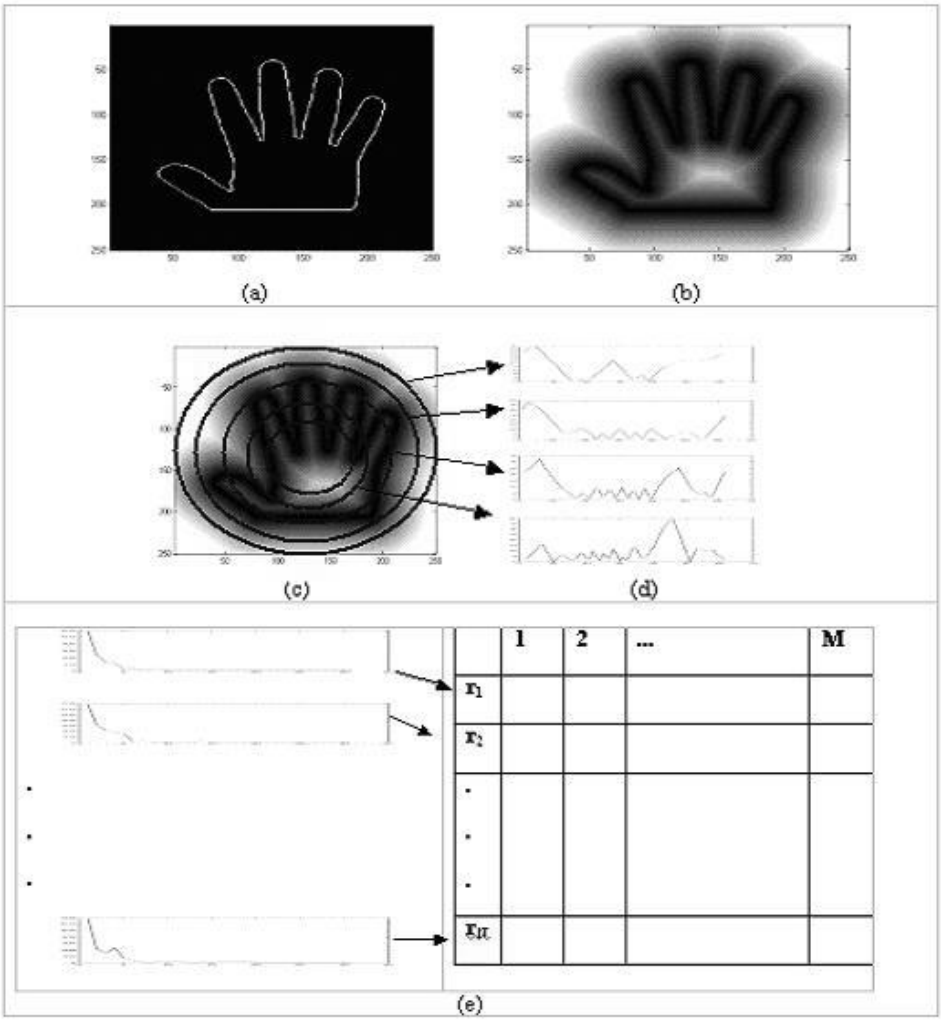

Figure 6. a, b) Contour of a hand and its distance transform defined on the plane. **c, d)** Concentric spheres on the distance transform and extracted profiles on circles. **e)** Feature extraction: DFTs of the circular profile of the distance transform function and the selected coefficients.

4. EXPERIMENTAL RESULTS

The hand database consisted of triple images of 458 individuals, in total 1374 images. The images, acquired with HP Scanjet 5300c scanner, were at 45 dpi resolution. There were no control pegs to orient the fingers, and there were no restrictions on hand accessories, like rings. During the three separate scan sessions the subjects could add or remove, at will, rings, or roll up or down sleeves. Two of these images were used as training, one for testing. Thus if we label the hand image sets as A, B, C, then the ordering of the test and training sets were {(A, BC), (B, AC), (C, AB)}.

Switching the set to be tested we conduct three experiments, i.e. the ordering of the test and training sets were {(A, BC), (B, AC), (C, AB)}, e.g., hands in the test set A were recognized using hands both in the sets B and C. Table 1 gives the average identification performance of these three experiments with respect to number of features. Average identification and verification performances versus increasing population size are listed in Tables 2 and 3.

Table 1. Identification performance of feature types with different number of selected features (population size: 458)

	Number of features			
Feature type	**40**	**100**	**200**	**400**
ICA_shape	94.32	97.67	98.4	97.31
ICA_appearance	95.41	**98.25**	**99.49**	**99.36**
PCA_shape	96.01	96.97	97.19	97.16
PCA_	**96.27**	97.91	97.99	97.91
ART_shape	94.18	95.78	95.63	95.05
ART_appearance	95.92	97.38	97.67	97.60
Distance	93.38	95.49	95.71	95.99

Table 2. Identification performance of feature sets with increasing population size.
(Best feature dimension selected for each feature type)

	Population size			
Feature type	**40**	**100**	**200**	**458**
ICA_shape	99.19	99.09	98.55	98.40
ICA_appearance	**99.68**	**99.65**	**99.58**	**99.49**
PCA_shape	98.67	98.69	98.56	97.19
PCA_appearance	99.14	98.89	98.72	97.99
ART_shape	98.72	97.78	97.00	95.78
ART_appearance	99.28	98.72	98.06	97.67
DT	99.17	98.22	96.22	95.99

Table 3. Verification performance with feature sets with increasing population size.
(Every feature set optimized with respect to the number of selected features. Equal Error Rate results are listed)

	Population size			
Feature type	**40**	**100**	**200**	**458**
ICA_shape	97.49	**98.97**	99.41	99.45
ICA_appearance	97.94	98.93	**99.49**	**99.74**
PCA_shape	98.27	97.80	97.83	97.78
PCA_appearance	**98.61**	98.50	98.73	98.49
ART_shape	98.29	97.89	97.95	97.91
ART_appearance	97.50	97.28	97.36	97.51
DT	98.31	98.03	98.08	98.34

We have also tested the case where there was a lapse of six months between training and testing acquisition times. We have selected ICA-based features, since they give superior results. The performance drops down significantly, especially in the case of shape-only recognition, as in Table 4. However this loss is mostly recuperated when textured hands are used, in which case the performance climbs back to just 1 percentage point below its level in Table 4. Figure 7 shows the genuine and imposter distributions with time lapses. The steep histogram at the origin represents the feature vector distances for genuines recorded minutes apart. The histogram below it represents distances for genuines six months apart. The histogram concentrated around distance point of 0.7 represents the distances of the impostors.

Table 4. Comparison of mean identification/verification performances with ICA features for sessions taken within minutes and with a time lapse of 6 months (47 people, 2 train - 1 test set)

	Identification (2 minutes apart)	**Identification (6 months apart)**	**Verification (2 minutes apart)**	**Verifiaction (6 months apart)**
ICA2 (shape)	97.87	97.87	99.81	99.58
ICA2 (appearance)	100.00	98.75	100.00	99.95

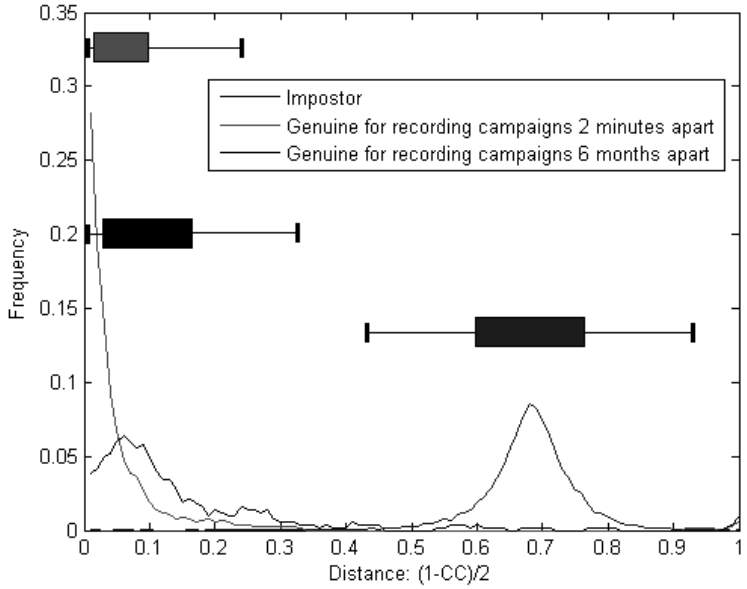

Figure 7. The genuine and imposter distributions with time lapses. The steep histogram at the origin represents the feature vector distances for genuines recorded minutes apart. The histogram below it represents distances for genuines six months apart. The histogram concentrated around distance point of 0.7 represents the distances of the impostors.

5. CONCLUSION

The novel algorithm hand-biometric algorithm has been observed to perform very well identification and verification tasks for an enrollment size of about 500. The critical importance of a proper registration that addresses both global and local differences has been shown. Several feature schemes are comparatively evaluated, and the Independent

Component Features are found to perform uniformly superior to all other features considered. The attained performance is 99.59% correct identification and of 99.74% EER verification for a population of 458 subjects. The effect of the time lapse time has been assessed. As training and test acquisition interval becomes of the order of several months, there is a few percentage point drop in performance. The complementary role of hand biometry in a multimodal application remains to be investigated.

6. REFERENCES

1. A.K. Jain, A. Ross, S. Prabhakar, "An Introduction to Biometric Recognition", IEEE Trans. Circuits and Systems for Video Technology, 14(1), 4-20, 2004.
2. R.L. Zunkel, "Hand Geometry Based Verification", pp. 87-101, in Biometrics, Eds. A. Jain, R. Bolle, S. Pankanti, Kluwer Academic Publishers, 1999.
3. A.K. Jain, A. Ross and S. Pankanti, "A prototype hand geometry based verification system", Proc. of 2nd Int. Conference on Audio- and Video-Based Biometric Person Authentication, pp. 166-171, March 1999.
4. A.K. Jain and N. Duta, "Deformable matching of hand shapes for verification, Proc. of Int. Conf. on Image Processing, October 1999.
5. R. Sanches-Reillo, C. Sanchez-Avila, and A. Gonzalez-Marcos, "Biometric Identification through Hand Geometry Measurements," *IEEE Transactions of Pattern Analysis and Machine Intelligence*, Vol. 22, No. 10, October 2000.
6. Y. Bulatov, S. Jambawalikar, P. Kumar and S. Sethia, "Hand recognition using geometric classifiers", DIMACS Workshop on Computational Geometry, Rutgers University, Piscataway, NJ, November 14-15, 2002.
7. C. Öden, A. Erçil and B. Büke, "Combining implicit polynomials and geometric features for hand recognition", Pattern Recognition Letters, 24, 2145-2152, 2003. .
8. D. Zhang and W. Shu, "Two novel characteristics in palmprint verification: datum point invariance and line feature matching", Pattern Recognition, 32, 691-702, 1999.
9. J. You, W. Li and D. Zhang, "Hierarchical palmprint identification via multiple feature extraction", Pattern Recognition 35(4), 847-859, 2002.
10. N. Duta, Anil K. Jain and K. V. Mardia, "Matching of palmprints", Pattern Recognition Letters 23(4), 447-485, February 2002
11. D. Zhang, W. K. Kong, J. You, and M. Wong, "Biometrics - Online palmprint identification," *IEEE Transactions on Pattern Analysis and Machine Intelligence*, 25(9), 1041-1050, 2003.
12. C.C. Han, H. L. Cheng, C. L. Lin, and K. C. Fan, "Personal authentication using palm print features," *Pattern Recognition* 36(2003), 371-381.
13. A. W. Kong, D. Zhang and W. Li, "Palmprint feature extraction using 2-D Gabor filters", Pattern Recognition 36(10), 2339-2347, 2003.
14. A. Kumar, D. C. M. Wong, H. C. Shen and A. K. Jain, "Personal Verification Using Palmprint and Hand Geometry Biometric", Proc. of AVBPA, pp. 668-678, Guildford, UK, June 9-11, 2003.
15. E. Yoruk, E. Konukoğlu, B. Sankur, J. Darbon, "Shape-Based Hand Recognition," *submitted to* IEEE Image Processing, 2004. Available at http://busim.ee.boun.edu.tr/sankur/
16. T. F. Cootes and C. J. Taylor, "Statistical models of appearance for computer vision", Technical Report, University of Manchester, 2000.
17. T. F. Cootes, G. J. Edwards, and C.J. Taylor, "Active appearance models," *IEEE PAMI*, Vol.23, No.6, pp.681-685, 2001.
18. B. A. Draper, K. Baek, M. S. Bartlett, and J. R. Beveridge, "Recognizing faces with PCA and ICA," *Computer Vision and Image Understanding*, 91 (1-2), 115-137, 2003.
19. A. Hyvarinen and E. Oja, "Independent component analysis: Algorithms and applications," *Neural Networks* 13 (4-5), 411-430, 2000.
20. S. Jeannin, "Mpeg-7 Visual part of eXperimentation Model Version 9.0", in ISO/IEC JTCI/SC29/WG11/N3914, 55th Mpeg Meeting, Pisa, Italia, Jan. 2001.
21. T. Funkhouser, P. Min, M. Kazhdan, J. Chen, A. Halderman and D. Dobkin, "A Search Engine for 3D Models", ACM Transactions on Graphics, vol. 22, No. 1, Jan. 2003.